

Three-Dimensional Protein Networks Assembled by Two-Photon Activation**

Volker Gatterdam, Radhan Ramadass, Tatjana Stoess, Manuela A. H. Fichte, Josef Wachtveitl, Alexander Heckel, and Robert Tampé*

Abstract: Spatial and temporal control over chemical and biological processes plays a key role in life and material sciences. Here we synthesized a two-photon-activatable glutathione (GSH) to trigger the interaction with glutathione *S*-transferase (GST) by light at superior spatiotemporal resolution. The compound shows fast and well-confined photo-conversion into the bioactive GSH, which is free to interact with GST-tagged proteins. The GSH/GST interaction can be phototriggered, changing its affinity over several orders of magnitude into the nanomolar range. Multiplexed three-dimensional (3D) protein networks are simultaneously generated *in situ* through two-photon fs-pulsed laser-scanning excitation. The two-photon activation facilitates the three-dimensional assembly of protein structures in real time at hitherto unseen resolution in time and space, thus opening up new applications far beyond the presented examples.

Chemical biology aims at controlling protein interactions and cell behavior by external stimuli.^[1] For this reason, research in the life sciences requires methods to organize and manipulate biomolecules in three dimensions (3D). Light is considered to be the optimal tool to create bioactive patterns of biomolecules. Key advantages are high temporal and spatial resolution combined with the ability to control the level of activation by the photon intensity or wavelength. Light is compatible with cells, tissues, and live animals. In

addition, further incubation or washing steps as in the case of small molecules, are not required. Recently, light-sensitive compounds have been described for the manipulation of biological systems,^[2] such as reversible photoswitches^[3] and one-way triggers,^[4] termed caged compounds.^[5] The generation of 2D structures is realized by photolithography,^[6] while the nonlinear two-photon effect can be used for 3D patterning.^[7] In the latter case, the target molecule must simultaneously absorb two photons to reach the excited state. The high photon density can be achieved by focusing a pulsed laser beam, typically at an excitation wavelength of twice the single-photon absorption maximum, with an objective lens of high numerical aperture. Recently, 3D structures of reactive

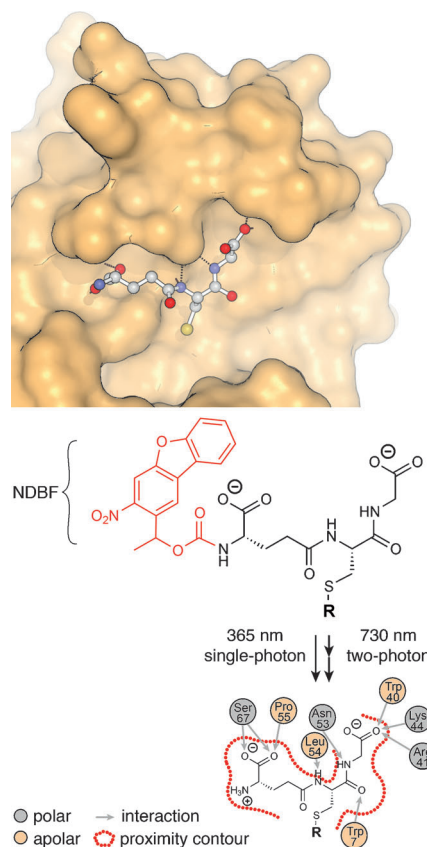


Figure 1. GSH/GST interaction triggered by light. GSH bound to GST (PDB 1UA5; *Schistosoma japonicum*) is shown as a surface representation (top) and interaction diagram (bottom). The novel two-photon-activatable GSH^{NDBF} can be converted into the bioactive GSH by photoactivation at 365 nm (single-photon) or 730 nm (two-photon). The thiol is used for modification with fluorophores or attachment to 2D and 3D matrices, indicated by the residue (R).

[*] Dr. V. Gatterdam, Prof. Dr. R. Tampé
Institute of Biochemistry, Biocenter
Goethe-University Frankfurt
Max-von-Laue-Strasse 9, 60438 Frankfurt am Main (Germany)
E-mail: tampe@em.uni-frankfurt.de
Homepage: <http://www.biochem.uni-frankfurt.de>
Dr. T. Stoess, M. A. H. Fichte, Prof. Dr. A. Heckel
Institute of Organic Chemistry and Chemical Biology
Goethe-University Frankfurt (Germany)
Dr. R. Ramadass, Prof. Dr. J. Wachtveitl
Institute of Physical and Theoretical Chemistry
Goethe-University Frankfurt (Germany)

[**] We thank Dr. Ralph Wieneke, Alina Kollmannsperger, and Christine Le Gal for helpful suggestions on the manuscript. The German Research Foundation (Cluster of Excellence—Macromolecular Complexes, SFB902, and SPP1623) supported the work. Tarmo Nuutinen and Dr. Juhani Syväoja (University of East Finland) provided the GST-eGFP vector. GST-(PA)mCherry was obtained from Dr. Jacob Piehler (University of Osnabrück (Germany)). We thank Dr. Niyas Yilmaz (Carl Zeiss Microscopy GmbH, Munich (Germany)) for generous support regarding the two-photon experiments.



Supporting information for this article is available on the WWW under <http://dx.doi.org/10.1002/anie.201309930>.

groups for the covalent coupling of biomolecules, and even the control of cell behavior, growth, and migration have been reported.^[1b,7a,8] However, these approaches are limited to sequential steps of reaction, incubation, and washing, which prevent protein assembly in situ. This drawback limits their applications for cellular systems.

The pseudo tripeptide glutathione (GSH) plays a pivotal role as a major redox regulator and scavenger of reactive oxygen species (ROS) in almost every cell.^[9] Together with the glutathione S-transferase (GST), GSH is involved in the xenobiotic detoxification of living organisms.^[10] The GSH/GST system is universally used for high-throughput and proteome-wide interaction screens,^[11] protein purification,^[12] and immobilization,^[13] making this generic interaction pair a prime target for a photoactivation approach.

Here, we describe a new and versatile approach for the 3D protein assembly by two-photon activation of GSH. We synthesized a two-photon-activatable GSH, masked with a nitrodibenzofuran (NDBF) group (GSH^{NDBF}) for advanced light-triggered applications. By using two-photon laser scanning microscopy, proteins were organized on demand in three dimensions with superior spatiotemporal resolution.

For efficient single-photon and multiphoton uncaging, the photolabile NDBF caging group^[14] was introduced at the amino terminus of the γ -L-glutamic acid. By photocleavage, GSH^{NDBF} is converted into bioactive GSH. Notably, this photoreaction can be triggered by single- as well as two-photon excitation (Figure 1). The key advantage of using the two-photon effect is a higher spatial resolution, in particular along the z-axis. Three-dimensional photoactivation occurs only in the high-photon flux region of the focal volume (ca. 1 fl).^[15] Less photodamage and light scattering, as well as a higher penetration depth for the long-wavelength light are further crucial benefits for non-invasive applications.

After a five-step synthesis of GSH^{NDBF} and characterization (see the Supporting Information), we followed the course of its photoreaction by reverse-phase (RP) C₁₈ HPLC (see Figure SI3). The photoactivation of GSH^{NDBF} follows a mono-exponential decay in direct relation to the mono-exponential formation of bioactive GSH. Notably, the photoactivation of GSH^{NDBF} is three times faster than that of the nitrophenylpropyl (NPP)-caged GSH (GSH^{NPP}), which is two-photon inactive.^[3d] We are aware that the primary photoreaction, which occurs within picoseconds, is followed

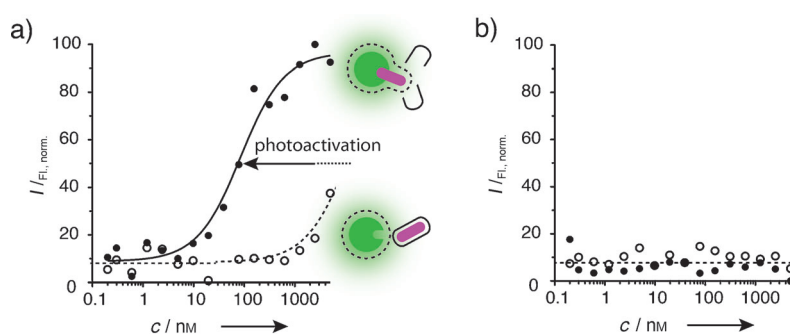


Figure 2. Light-triggered high-affinity GSH–GST complex formation analyzed by MST. The thermophoretic movement of GST–eGFP is detected due to the change in hydration shell, indicated by the dashed circles. a) GST–eGFP (5 nM) was incubated with increasing concentrations of caged (○) and photoactivated GSH^{NDBF} (●). For photoactivation, samples were illuminated at 365 nm (185 mWcm^{−2}) for 2 min resulting in $K_D = (82 \pm 19)$ nM. A low-affinity interaction was detected for the caged species. b) Experiment identical to that in (a) but with an excess of GSH (5 mM) as a competitor, demonstrating the specificity of the interaction.

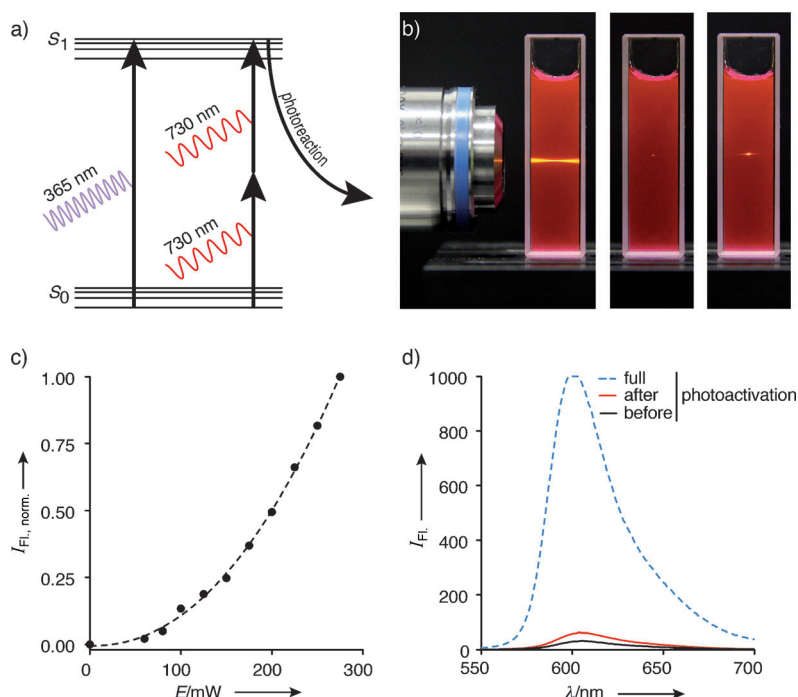


Figure 3. Two-photon effect and power dependency of the GSH^{NDBF} photoactivation. a) Jablonski diagram comparing the single- and two-photon excitation leading to a photoreaction. The two-photon activation is only possible in a spatially defined spot with high photon density. b) Illustration of the two-photon effect in a solution of Atto565-labeled GSH^{NDBF} (10 μ M). The single-photon (left) and two-photon excitation (middle) is illustrated using the same setup. An over-powered two-photon excitation leads to a loss in z-resolution (right). c) Change in fluorescence intensity of Atto565 after two-photon removal of the quenching NDBF group. Photoactivation was performed with a 730 nm infrared laser and different illumination intensities. Data were fitted using the equation $y = A + Bx^C$, where the parameter C for two-photon power dependence was found to be 2.17, confirming it to be a two-photon process. d) Fluorescence spectra of Atto565-labeled GSH at different time points during the experiment in (c). The results demonstrate that less than 3% of the total GSH^{NDBF} population was photoactivated and that the total concentration of GSH^{NDBF} did not significantly change during the experiment.

by a slower decarboxylation in the micro- to millisecond range.^[16] The uncaging efficiency—defined as the product $\epsilon\phi$ of the molar absorption coefficient and the quantum yield for the uncaging process—was determined to be $1600 \text{ L mol}^{-1} \text{ cm}^{-1}$ for GSH^{NDBF} and $100 \text{ L mol}^{-1} \text{ cm}^{-1}$ for GSH^{NPP} .^[17] Similar tendencies had been found before for caged oligonucleotides.^[18]

We next analyzed the light-induced interaction between GSH and GST-tagged enhanced green fluorescent protein (GST-eGFP) by microscale thermophoresis (MST). Before photoactivation, only a very weak interaction was detected (Figure 2a). After photoactivation, a high-affinity interaction with $K_D = (82 \pm 19) \text{ nm}$ was determined, which can be blocked by an excess of GSH (Figure 2b). In parallel, we established a Förster resonance energy transfer (FRET) assay using GST-eGFP and GSH^{NDBF} labeled with Atto565 as a fluorescence donor–acceptor pair. The FRET analysis yielded a very weak $K_D > 4 \mu\text{M}$ before and $K_D = (0.28 \pm 0.02) \mu\text{M}$ after illumination (see Figure SI5).

To provide direct evidence for the two-photon process, GSH^{NDBF} labeled with Atto565 was photoactivated at 730 nm by fs-pulsed laser excitation (Figure 3). As a notable side effect, the fluorophore is quenched by the NDBF caging group, most likely due to contact quenching or photoinduced electron transfer (PET).^[19] Thus, we followed the photoactivation of GSH^{NDBF} directly by unquenching of the fluorophore. Notably, the fluorescence showed a near quadratic power dependence towards the laser power at 730 nm, which provides formal proof for a two-photon process (Figure 3c). The two-photon cross-section of the NDBF core chromophore had been determined to be $0.6 \times 10^{-50} \text{ cm}^4 \text{ s}^{-1} \text{ photon}^{-1}$ (0.6 Goeppert-Mayer) in the context of the Ca^{2+} -chelating NDBF-EGTA (ethyleneglycol bis(2-aminoethyl)ether tetraacetic acid).^[14] As a control, fluorescence spectra were recorded at every time point of the experiment to confirm a negligible consumption of the caged compound (Figure 3d).

To demonstrate the assembly of GST-tagged proteins by light, we followed two different approaches. Mask lithography was used to photoactivate large surfaces functionalized with GSH^{NDBF} and biocompatible polyethylene glycol. After binding of GST-eGFP or GST-photoactivatable (PA)mCherry, protein patterns were monitored by confocal laser-scanning microscopy (CLSM). GST-eGFP was assembled in well-defined protein patterns, even in the presence of the competing cell lysate of *E. coli*, demonstrating the specificity of the light-triggered interaction (Figure 4a, Figure SI4). Photopatterning also confirmed that the protein assembly was three times faster (see Figure SI7).

We next used a 405 nm scanning laser to establish a freely designed assembly of proteins by light (Figure 3b–d). Efficient photoactivation occurs within several milliseconds to seconds, depending on the size of the written structure. Different protein densities were achieved by a variation of the laser power, reflecting a linear dependence at lower intensities (Figure 3b). A photoprinted QR-Code is shown as an example for a complex arrangement of GSH-tagged proteins (Figure 3c), attesting that even binary coded information can be stored in protein patterns. Furthermore, multiprotein

arrays were realized by repeating a second cycle of light activation and binding of a different protein (Figure 3d). In situ assembly of GST-tagged proteins was followed in real-time by CLSM (Figure 3e; SI Movie 1). After a short 405 nm scan (“write”: 2 s), the assembly of the GST-eGFP was followed by CLSM (“read”: 0–180 s). The in situ assembly of target proteins was fast and reached saturation already after a few seconds.

To demonstrate protein assembly in 3D by two-photon laser writing, we developed biocompatible and transparent

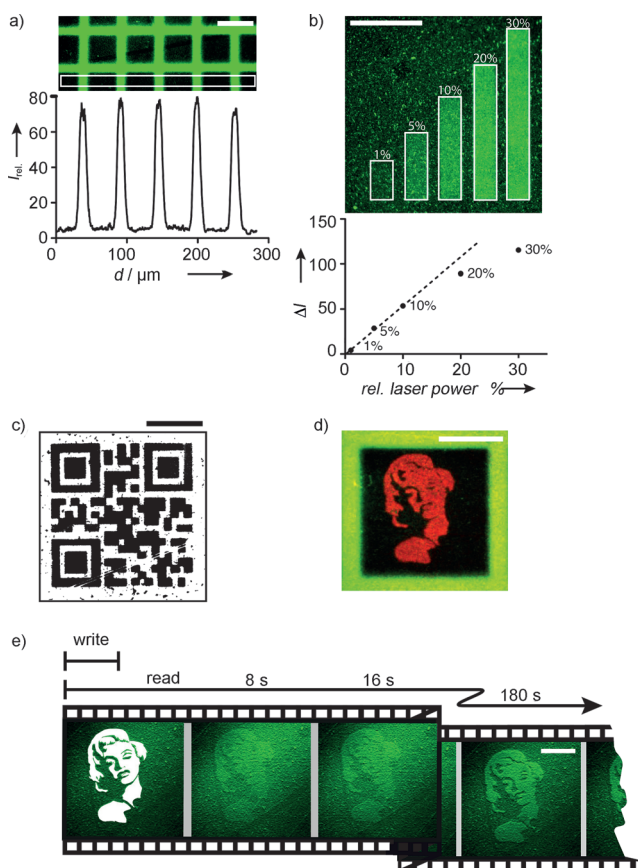


Figure 4. In situ protein assembly in 2D. a) Mask patterning of a grid structure using a 365 nm UV-LED system (75 mW cm^{-2} ; $2.3 \text{ mmol photons m}^{-2} \text{ s}^{-1}$) for 5 s. The intensity profile of the marked regions shows a superb contrast of illuminated and nonilluminated areas. A total cell lysate of *E. coli* expressing GST-eGFP was used for protein patterning. b) Variation of 405 nm laser intensity and the corresponding intensities of the light-activated areas. At low laser energies, a linear dependency between protein density and laser intensity is observed. c) Assembly of a complex structure such as a QR-Code by laser scanning. The image is converted into inverse gray scale for better decoding. The information stored codes for the word “glutathione”. d) The green frame was generated by mask patterning and incubation with *E. coli* cell lysate containing GST-eGFP. In a second round of GSH^{NDBF} activation, the image of Marilyn Monroe was written by laser scanning using GST-(PA)mCherry. e) In situ activation of caged GSH in the presence of GST-eGFP (500 nm). Photoactivation at 405 nm was performed for two seconds (“write”) followed by monitoring of the protein assembly by the GST-eGFP fluorescence (“read”). Already several seconds after photoactivation, the written structure can be visualized (see SI Movie 1). Scale bars are 50 μm in all images.

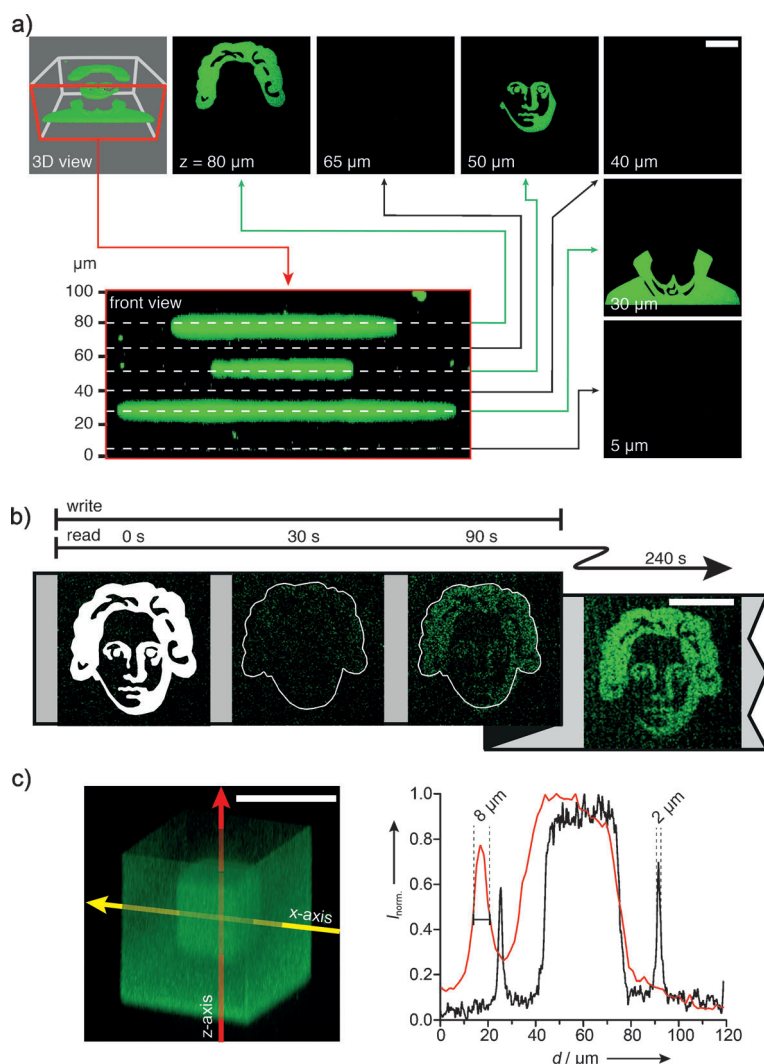


Figure 5. Building 3D protein networks by two-photon activation. GSH^{NDBF}-functionalized hydrogels were two-photon-activated and the image of Johann Wolfgang Goethe was written. a) 3D structures were visualized by assembly of GST-eGFP. Images were reconstructed from a series of z-stacks. b) In situ two-photon activation of GSH^{NDBF} and assembly of GST-eGFP (50 nm). The two-photon activation at 730 nm took 90 s at 7 mW laser intensity, while the eGFP fluorescence was recorded in parallel by spinning disc confocal microscopy (see SI Movie 3). For optimal visualization, the change in fluorescence is presented by subtraction of the background signal at time point zero. c) Cube pattern nested inside a patterned box. Intensity profiles of eGFP in x- and z-directions (black and red traces, respectively) are plotted on the right. The resolution (FWHM) measured at the bottom of the central box is 8 μm and 2 μm in the z- and x-directions, respectively. Scale bars are 50 μm in all images.

hydrogels functionalized with GSH^{NDBF} (see the Supporting Information). Desired 3D patterns were generated by two-photon activation at 730 nm using fs-pulsed scanning laser integrated in a confocal microscope setup, which allows the illumination of spatially well-defined areas. The formation of 3D protein networks was monitored either after washing or directly in real time during the in situ protein assembly. The organization of proteins in 3D with a high signal-to-background ratio is shown in Figure 5a and SI Movie 2. Depending on the volume of activation, the illumination time was in

the second to minute range. Multiplexing and 3D assembly of different target proteins was achieved by the consecutive binding of GST-eGFP and GST-(PA)mCherry (SI Movie 3). Finally, in situ two-photon activation and real-time 3D assembly were achieved in the presence of GST-eGFP (Figure 5b; SI Movie 4). Simultaneous photoactivation and fluorescence monitoring identified protein clustering emerging already 1 min after two-photon activation. Two-photon activation leads to a z-resolution of 8 μm (FWHM), showing a resolution close to the theoretical limit (Figure 5c). This approach allows the activation and in situ protein assembly in a fast and direct way.

In conclusion, protein interactions can be triggered by two-photon activation with superior spatiotemporal resolution using the new GSH^{NDBF}. The caged GSH^{NDBF} displays a fast and well-defined photoconversion. The affinity of the GSH/GST interaction pair can be phototriggered over several orders of magnitude into the nanomolar range. Through the use of biocompatible hydrogels, 3D protein networks were assembled under physiological conditions in competing cell lysates by fast photoactivation at defined regions of interest. For the first time, to our knowledge, protein networks can be assembled by two-photon activation and followed in real time without any intermediate processing. Based on the generic function and broad use of the GSH/GST interaction pair, this optochemical approach can facilitate future applications in cell guidance and development. The feasibility of the hydrogel approach is shown by the work of DeForest and Anseth.^[20] Through two-photon laser activation, membrane-associated receptors or adhesion molecules can be organized and clustered in living cells embedded in hydrogels. In this way, signaling pathways can be triggered on demand by light and probed with previously unmatched resolution in time and space. Cell adhesion, morphology, and networking may be guided by the in situ “photo-writing” of responsible cellular factors, which are currently under investigation.

Received: November 15, 2013

Revised: January 23, 2014

Published online: April 11, 2014

Keywords: immobilization · photochemistry · protein–protein interactions · surface chemistry · two-photon activation

- [1] a) R. G. Wylie, S. Ahsan, Y. Aizawa, K. L. Maxwell, C. M. Morshead, M. S. Shoichet, *Nat. Mater.* **2011**, *10*, 799–806; b) C. A. DeForest, K. S. Anseth, *Nat. Chem.* **2011**, *3*, 925–931.
- [2] G. Bort, T. Gallavardin, D. Ogden, P. I. Dalko, *Angew. Chem.* **2013**, *125*, 4622–4634; *Angew. Chem. Int. Ed.* **2013**, *52*, 4526–4537.

- [3] a) R. H. Kramer, J. J. Chambers, D. Trauner, *Nat. Chem. Biol.* **2005**, *1*, 360–365; b) P. Gorostiza, E. Y. Isacoff, *Science* **2008**, *322*, 395–399; c) A. A. Beharry, G. A. Woolley, *Chem. Soc. Rev.* **2011**, *40*, 4422–4437; d) V. Gatterdam, T. Stoess, C. Menge, A. Heckel, R. Tampé, *Angew. Chem.* **2012**, *124*, 4027–4030; *Angew. Chem. Int. Ed.* **2012**, *51*, 3960–3963.
- [4] a) A. P. Pelliccioli, J. Wirz, *Photochem. Photobiol. Sci.* **2002**, *1*, 441–458; b) X. Tang, I. J. Dmochowski, *Mol. Biosyst.* **2007**, *3*, 100–110; c) C. Grunwald, K. Schulze, A. Reichel, V. U. Weiss, D. Blaas, J. Piehler, K. H. Wiesmuller, R. Tampé, *Proc. Natl. Acad. Sci. USA* **2010**, *107*, 6146–6151; d) N. Labòria, R. Wieneke, R. Tampé, *Angew. Chem.* **2013**, *125*, 880–886; *Angew. Chem. Int. Ed.* **2013**, *52*, 848–853.
- [5] a) G. C. Ellis-Davies, *Nat. Methods* **2007**, *4*, 619–628; b) H. M. Lee, D. R. Larson, D. S. Lawrence, *ACS Chem. Biol.* **2009**, *4*, 409–427; c) G. Mayer, A. Heckel, *Angew. Chem.* **2006**, *118*, 5020–5042; *Angew. Chem. Int. Ed.* **2006**, *45*, 4900–4921.
- [6] a) J. D. Hoff, L. J. Cheng, E. Meyhofer, L. J. Guo, A. J. Hunt, *Nano Lett.* **2004**, *4*, 853–857; b) D. Ryan, B. A. Parviz, V. Linder, V. Semetey, S. K. Sia, J. Su, M. Mrksich, G. M. Whitesides, *Langmuir* **2004**, *20*, 9080–9088.
- [7] a) S. H. Lee, J. J. Moon, J. L. West, *Biomaterials* **2008**, *29*, 2962–2968; b) J. Fischer, M. Wegener, *Laser Photonics Rev.* **2013**, *7*, 22–44.
- [8] Y. Luo, M. S. Shoichet, *Nat. Mater.* **2004**, *3*, 249–253.
- [9] V. B. Djordjevic, *Int. Rev. Cytol.* **2004**, *237*, 57–89.
- [10] J. D. Hayes, L. I. McLellan, *Free Radical Res.* **1999**, *31*, 273–300.
- [11] a) K. R. Bhushan, *Org. Biomol. Chem.* **2006**, *4*, 1857–1859; b) J. W. Jung, S. H. Jung, H. S. Kim, J. S. Yuk, J. B. Park, Y. M. Kim, J. A. Han, P. H. Kim, K. S. Ha, *Proteomics* **2006**, *6*, 1110–1120.
- [12] D. B. Smith, K. S. Johnson, *Gene* **1988**, *67*, 31–40.
- [13] C. M. Kolodziej, C.-W. Chang, H. D. Maynard, *J. Mater. Chem.* **2011**, *21*, 1457–1461.
- [14] A. Momotake, N. Lindegger, E. Niggli, R. J. Barsotti, G. C. Ellis-Davies, *Nat. Methods* **2006**, *3*, 35–40.
- [15] a) W. Denk, J. H. Strickler, W. W. Webb, *Science* **1990**, *248*, 73–76; b) G. C. Ellis-Davies, *ACS Chem. Neurosci.* **2011**, *2*, 185–197.
- [16] a) G. Papageorgiou, J. E. T. Corrie, *Tetrahedron* **1997**, *53*, 3917–3932; b) A. G. Russell, M. E. Ragoussi, R. Ramalho, C. W. Wharton, D. Carteau, D. M. Bassani, J. S. Snaith, *J. Org. Chem.* **2010**, *75*, 4648–4651; c) J. E. Corrie, V. R. Munasinghe, D. R. Trentham, A. Barth, *Photochem. Photobiol. Sci.* **2008**, *7*, 84–97.
- [17] Quantum yields of the photoactivation were determined to be 0.15 for GSH^{NDBF} and 0.34 for GSH^{NPP}.
- [18] F. Schäfer, K. B. Joshi, M. A. Fichte, T. Mack, J. Wachtveitl, A. Heckel, *Org. Lett.* **2011**, *13*, 1450–1453.
- [19] S. Doose, H. Neuweiler, M. Sauer, *ChemPhysChem* **2009**, *10*, 1389–1398.
- [20] C. A. DeForest, K. S. Anseth, *Angew. Chem.* **2012**, *124*, 1852–1855; *Angew. Chem. Int. Ed.* **2012**, *51*, 1816–1819.